Article:
Lee, W.H., Pandhal, J., Roy, I. et al. (2026) Compatibilization and reinforcement of PHB/PBAT bends via sequential blending of surface-modified cellulose. Polymer Engineering & Science. ISSN: 0032-3888

https://doi.org/10.1002/pen.70587

Polymer Engineering & Science

WILEY | spe INSPIRING PLASTICS PROFESSIONALS

RESEARCH ARTICLE OPEN ACCESS

Compatibilization and Reinforcement of PHB/PBAT Blends via Sequential Blending of Surface-Modified Cellulose

Wai Hin Lee[1] | Jagroop Pandhal[2] | Ipsita Roy[2] | Chaoying Wan[1]

[1]International Institute for Nanocomposites Manufacturing (IINM), WMG, University of Warwick, Coventry, UK | [2]School of Chemical, Materials & Biological Engineering, University of Sheffield, Sheffield, UK

Correspondence: Chaoying Wan (chaoying.wan@warwick.ac.uk)

Received: 3 December 2025 | **Revised:** 25 April 2026 | **Accepted:** 29 April 2026

Keywords: biodegradable polymers | mechanical analysis | reactive processing | sequential blending | surface modification

ABSTRACT

Polyhydroxybutyrate (PHB) is a natural and biodegradable polymer generated by bacteria. While its applications to potentially replace petroleum-based plastics are severely limited due to its brittleness and notoriously low thermal stability. In this work, biodegradable composites of PHB/poly(butylene-adipate terephthalate) (PBAT) and cellulose are prepared via reactive melt-processing with a chain extender of epoxy-functional polymer. The effects of blending sequence on the morphology, rheological and mechanical properties of the composites are investigated. Commercial cellulose fiber is pre-modified with stearic acid to improve its compatibility with the polymers. The melt-processing conditions of PHB/PBAT (70/30 w/w) blend were first optimized by minimizing PHB thermal degradation. Then two processing methods were conducted, (i) one-step batch blending of PHB/PBAT/cellulose, and (ii) sequential blending of PBAT/cellulose, then blending with PHB. It is found that the sequential blending method facilitated the dispersion of PBAT/cellulose in the PHB matrix and improved the toughness of the composite without compromising the elongation, as compared to the one-step blended counterpart. The preferential location of cellulose fiber in PBAT effectively facilitates energy dissipation of the toughening PBAT phase. This work demonstrates an avenue to optimize the mechanical properties and thermal stability of polymer blends and composites by carefully altering the blending sequence without the need of excessive additives.

1 | Introduction

Polyhydroxybutyrate (PHB) is a natural polymer generated by bacteria as a form of energy storage and therefore has long been considered a sustainable alternative to petroleum-based plastic due to its bioavailability and degradability. PHB was first extracted and characterized in the 1920s [1]. However, its application is still limited despite numerous early attempts to improve its processing and even commercialization [2–6]. The challenges include its inherent brittleness and low thermal stability at processing temperature [7, 8]. To address this, reactive processing with a chain extender such as multifunctional epoxy, isocyanate, hyperbranched polymer is usually adopted to improve the thermal stability against degradation [9–11]. During reactive processing, degraded low molecular weight fragments are captured with these reactive moieties from chain extenders and regenerate high molecular weight species.

The second advantage of reactive processing is that the chain extender also in situ generates copolymer as a compatibilizer when PHB is blended with a second soft material to toughen the material. This strategy has been widely used in PLA/PBAT blend, namely Ecovio by BASF, to make compostable packaging [12]. Javadi et al. initially prepared PHBV/PBAT blend without any compatibilizer but the properties are poor even with up to 50% PBAT content [13]. Misra et al. later extensively investigated the reactive processing of PHBV/PBAT with triallyl isocyanurate via radical grafting

Highlights

- Hard/soft polymer blend of PHB/PBAT to mitigate the brittleness of PHB.
- Reactive processing to overcome thermal degradation and compatibilize PHB/PBAT blend.
- Novel numerical analyses of tensile tests on polymer blends.
- Surface modification of cellulose fiber to selectively disperse in PBAT phase.
- Sequential blending further reinforced PHB/PBAT blend by 50% as compared to the one-step batch mixing method.

reaction, and achieved significant improvements in elongation and toughness by 1000% and 200%, respectively [14, 15].

Cellulose is another abundantly sourced biopolymer and it is also the main component in plant fibers. Cellulose fiber (e.g., bamboo, hemp) is widely used as a reinforcement or filler in biopolymers to make natural composite materials. However, owing to the highly crystalline structure and surface hydroxy groups, cellulose is incompatible with PHA, thus surface modification is required to enhance the adhesion of polymer onto the fiber to attain reinforcement [16, 17]. While chemicals like acyl chloride [18–20] or anhydride [21, 22] are known to be efficient in surface modification of cellulose, the chemical itself is highly hazardous which opposes the purpose of cellulose as a sustainable reinforcement. Alkyl ketene dimer is a safe alternative to enhance the hydrophobicity of cellulose and is widely used in the paper industry as a sizing agent [23, 24]. The moderate reactivity allows its storage as an emulsion and is only activated upon drying at elevated temperatures. Steglich esterification is the simplest and direct route to modify cellulose by suspending the fiber in the desired carboxylic acid mixture to synthesize various cellulose ester [25–28]. The advantage of direct esterification is that by adjusting the temperature, acid/cellulose ratio or reaction time, different degrees of modification and exfoliation can be attained.

Sequential blending is a method to selectively localize filler or additive in composite materials during processing. Due to the combination of surface wettability, particle transportation and partition, polymer phase separation, the microstructure and dispersion are altered by the blending sequence and thus the properties can be drastically different from those prepared by one-step batch blending [29, 30]. Pal et al. found that preparation of organo-modified clay in PBAT masterbatch improved dispersion of clay in the PBAT/PHBV blend [14]. Siegmann et al. prepared electrical-conductive composite of carbon black-filled nylon/polypropylene by sequentially blending carbon black first into polypropylene, then to nylon. This forces the carbon black to migrate from less-prefered polypropylene phase to the interfaces, thus lowers the percolation threshold to 2% carbon black loading [31]. Yu et al. observed the opposite effect in the reactive processing of carbon nanotube (CNT) reinforced polyamide/polypropylene-maleic anhydride (PA/PP-MAH) copolymer, where complete aggregation was observed in PP-MAH/CNT masterbatch while percolated CNT formed in PA/CNT masterbatch [32].

In this work, we systematically optimized the blending process of PHB/PBAT to mitigate thermal degradation and phase separation with the aid of Joncryl ADR 4486 as chain extender and compatibilizer. We also prepared stearic acid modified cellulose fiber to improve its dispersion in the hydrophobic PBAT phase selectively. Then we evaluated the effects of mixing sequence on rheology, mechanical properties, and microstructure of the polymer composites, and demonstrated the enhanced reinforcement via sequential blending even from the same composition.

2 | Experimental

2.1 | Materials

Microcrystalline cellulose (MCC, cotton linter, powder, 20 μm), stearic acid (SA, 95%), and acetic anhydride are supplied by Sigma-Aldrich. Sulfuric acid (98%) and 2-propanol are purchased from Fisher Scientific. Joncryl ADR 4468 (MW: 7250 g mol^{-1}, epoxy equivalent weight: 310 g mol^{-1}) is supplied by BASF. P209 PHB is purchased from Biomer, and Ecoflex C1220 poly(butanediol-adipate-terephthalate) is purchased from BASF.

3 | Preparation

3.1 | Modification of Cellulose Fiber With Stearic Acid (MCCSA)

In a typical experiment, SA (52.7 g) was melted at 130°C. Acetic anhydride (5.8 mL) and 3 drops of sulfuric acid as a catalyst were added. MCC (10.0 g) was lastly added to prevent its combustion due to locally concentrated sulfuric acid. The reaction was allowed to proceed for 3 h and terminated by cooling down to freeze at ambient conditions. The solid mixture containing acetic acid, stearic acid, and cellulose fiber was subjected to Soxhlet extraction with 2-propanol for 48 h to remove the excess stearic acid, residual acid, and the derivatives from oxidized cellulose. The remaining solid was dried in a vacuum oven overnight to remove 2-propanol and stored at ambient conditions until use.

3.2 | Polymer Processing

For PHB/PBAT blend, cryo-milled PHB (10.5 g) and PBAT (4.5 g) were premixed with Joncryl ADR 4468 (0/0.15/0.3/0.45 g) and added into Thermo MiniLab twin-screw compounder. Samples were extruded at 180°C and 100 min^{-1} rotation speed for 3 times with a total retention time of approximately 5 mins.

For PBAT-cellulose masterbatch, PBAT was premixed with stearic acid-modified MCC powder (MCCSA) with weight ratio of 9:1 or 3:1 w/w, and melt-processed under the same condition as shown above.

For one-step batch mixing of PHB/PBAT/MCCSA composite, cryo-milled PHB (10.5 g), PBAT (4.5 g) and MCCSA (0.45/1.5 g) were premixed with Joncryl ADR 4468 (0.3 g). For sequential blending, 9:1 w/w PBAT/MCCSA (4.95 g) and 3:1 w/w

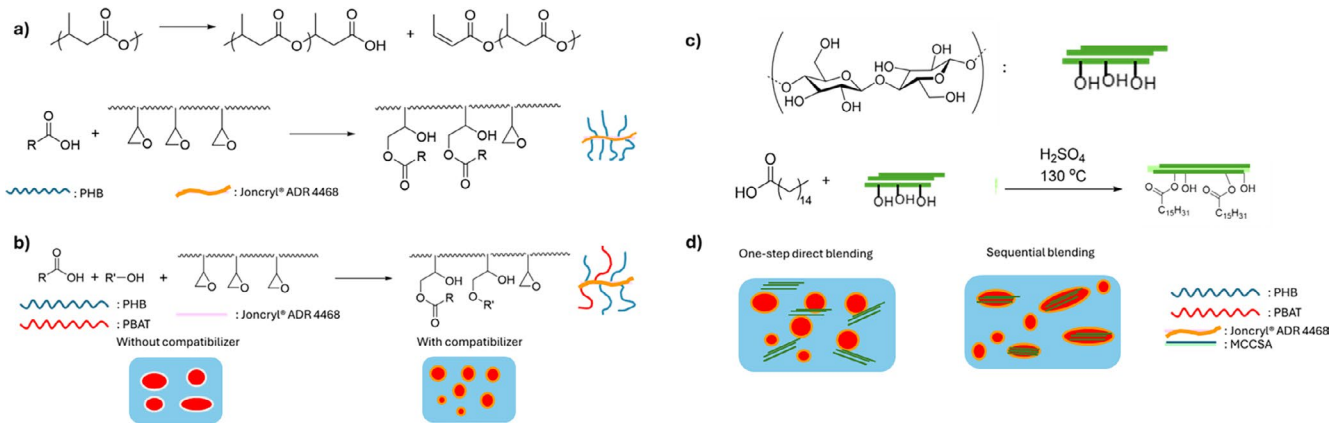

SCHEME 1 | Illustration of the preparation of biodegradable PHB/PBAT/cellulose composite in this work. (a) thermal degradation of PHB and its suppression by Joncryl ADR 4468; (b) in situ formation of grafted copolymer by Joncryl ADR 4468 to compatibilize immiscible polymer blend; (c) reaction scheme of esterification of cellulose fiber with stearic acid; (d) Comparsion of proposed phase separation mechanisms in one-step blending and sequential blending of PHB/PBAT/cellulose composites.

PBAT/MCCSA (6 g) were pre-mixed then blended with PHB, Nomenclature is designated as PHB/PBAT/x-MCCSA for one-step batch blending and PHB/(PBAT/x-MCCSA) for sequential blending of PBAT/MCCSA masterbatch with x % of MCCSA in final composites. All the blends and composites were melt-processed under the same conditions as shown above.

4 | Characterization

Infrared spectroscopy is performed on the Bruker Tensor 27 FT-IR Spectrometer. For each sample, 32 scans of 4000–400 cm^{-1} with resolution of 2 cm^{-1} were acquired in transmittance mode at ambient conditions. The spectrum was baseline corrected and normalized.

Thermogravimetric analysis is performed on the Mettler Toledo Thermogravimetric Analyzer. The weighed sample was loaded in an open alumina crucible and subjected to heating from 40°C to 600°C at 10°C min^{-1} under a constant nitrogen flow.

Differential scanning calorimetry is performed on Mettler Toledo DSC1. The weighed sample was loaded in a pin-holed aluminium pan and subjected to 3 cycles of heating to 200°C then cooling to −50°C at 15°C min^{-1} under a constant nitrogen flow. Crystallinity is calculated from the integration of the heat flux versus temperature in the 2nd cooling cycle (crystallization) and the 3rd heating cycle (melting) relative to the pristine PHB as received. Example of pristine PHB was shown in Figure S1. Polymer processing is performed on Thermos MiniLab twin-screw extrusion. Samples were extruded at 180°C and 100 min^{-1} rotation speed for 3 times with a total retention time of approximately 5 min.

Hot pressing was performed on collin hot press. Extruded sample was loaded in a square mold of 120 × 120 × 1 mm^3 then subjected to a thermal profile of 180°C and 150 bar for 3 min then cooling from 180°C to 50°C at 15°C min^{-1} and held at 50°C for an additional 15 min. Tensile specimen was cut with Montech die cutter with the geometry according to ISO 527-3 for tensile testing.

Scanning electronic microscopy is performed on TESCAN CLARA SEM equipped with a detector using a working voltage of 3 kV. For MCC fiber, the sample was suspended in chloroform then drop cast on aluminium foil affixed to an aluminium stub with conductive carbon tape. For composite samples, a hot pressed sample 1 mm thick was submerged in liquid N_2 then fractured to expose the cross-section. All samples were sputtered with carbon prior to imaging.

Tensile test is performed on Shimadzu AGS-X using a 10 kN loading cell with parallel cross-hatched gripping plates. Tensile specimen was loaded and subjected to a uniaxial tension at a constant speed of 50 mm min^{-1}. Data processing of stress-strain curve was performed on Python 3.2.

Rheology was performed on Anton Paar MCR 302 rheometer equipped with Peltier parallel plates (diameter: 20 mm) and active N_2 flow cooling. Samples were loaded at 180°C and kept for 3 min until complete melting then trimmed to 20 mm diameter. The amplitude was set as 1% and the frequency was set from 0.1 rad s^{-1} to 1000 rad s^{-1} increasing logarithmically with 30 data points.

5 | Result and Discussion

This work first mitigates the thermal degradation of PHB during processing by adding Joncryl ADR 4468 epoxy-based copolymer as a chain extender; then incorporating PBAT to form compatibilized blend via reactive processing to improve the toughness. In parallel, cellulose fiber is modified with stearic acid to enhance its dispersion in PHB/PBAT blend. Finally, a biodegradable composite is prepared by sequential blending to investigate its effect on phase separation and mechanical properties (Scheme 1).

5.1 | Minimize Thermal Degradation of PHB With a Chain Extender

PHB is known to be thermally unstable even at its melting point via self-catalyzed retro-oxa Michael addition. By adding chain

extender Joncryl ADR 4468, the epoxy moieties react with the acid and/or hydroxy end groups of PHB to (i) form branched/crosslinked PHB to counter-balance the thermal degradation; and/or (ii) to capture the degraded PHB and regenerate high molecular weight PHB, which overall reduced the oligomeric species to maintain its high molecular weight and processibility. Figure 1 showed the molecular weight distribution of PHB directly dissolved from pellets, and after processing with 0,1,2,3% w/w chain extender. Without a chain-extender, M_n and M_w reduced from 62,100 to 17,300, and 165,700 to 42,800 respectively after processing (Table 1). With a chain-extender, the molecular weight of soluble fraction (fraction crosslinked by chain-extender was not soluble) remains equivalent to pristine PHB.

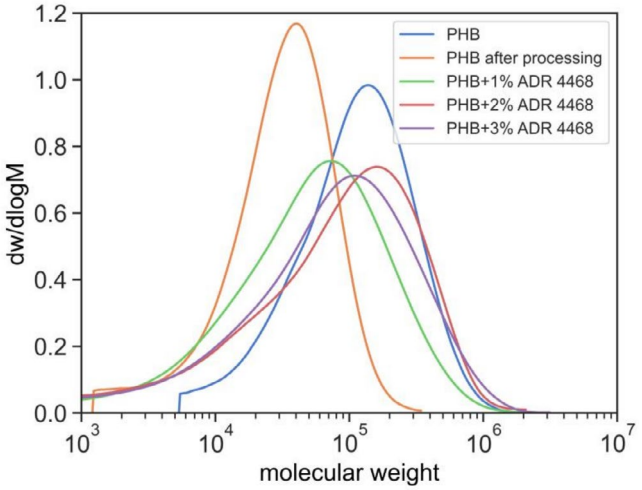

FIGURE 1 | Molecular weight distribution of pristine PHB (blue), processed PHB with 0 (orange), 1 (green), 2 (red), 3% w/w (purple) chain extender.

TABLE 1 | M_n, M_w, and dispersity of pristine PHB, processed PHB with 0%, 1%, 2%, and 3% w/w chain extender.

	$M_{n\ (g/mol)}$_	$M_{w\ (g/mol)}$	PDI
PHB	62,100	165,700	2.67
Melt-processed PHB	17,300	42,800	2.47
PHB+ 1% ADR	18,500	102,800	5.56
PHB+ 2% ADR	19,600	163,700	8.35
PHB+ 3% ADR	18,400	157,500	8.55

The effect of thermal degradation on the composite properties was evaluated by mechanical testing and rheology. The stress–strain curves and its derivative are shown in Figure 2. The Young's modulus, strain, ultimate strength, elongation at break, and toughness are summarized in Table 2. The thermal degradation of PHB increased its brittleness and rigidity, with the Young's modulus increasing from 226 MPa to 312 MPa, but the elongation at break falling from 31.05% to 12.41%, and the toughness from 3582 kPa to 1089 kPa. Similar weakening was observed when 1% Joncryl ADR 4486 was added, suggesting thermal degradation is still predominant.

At 2% Joncryl ADR 4486, the effect of chain extension significantly counterbalanced the thermal degradation with the Young's modulus of 320 MPa, elongation at back of 30.0%, and the toughness of 3925 kPa. Despite further improvement in toughness and elongation at break at 3% Joncryl ADR 4486 to 4703 kPa and 38.79%. The material was softened again with reduced Young's modulus and final toughness to 284 MPa and 14.6 MPa respectively, which was possibly due to the plasticization of oligomeric chain extender at increasing content.

The effect of thermal degradation with and without a chain-extender was compared in Figure 3. The viscosity of PHB was reduced by 18 times from 0.429 Pa s to 0.024 Pa s at 0.1 rad s^{-1}. We observed the viscosity rose sharply as it changed from laminar

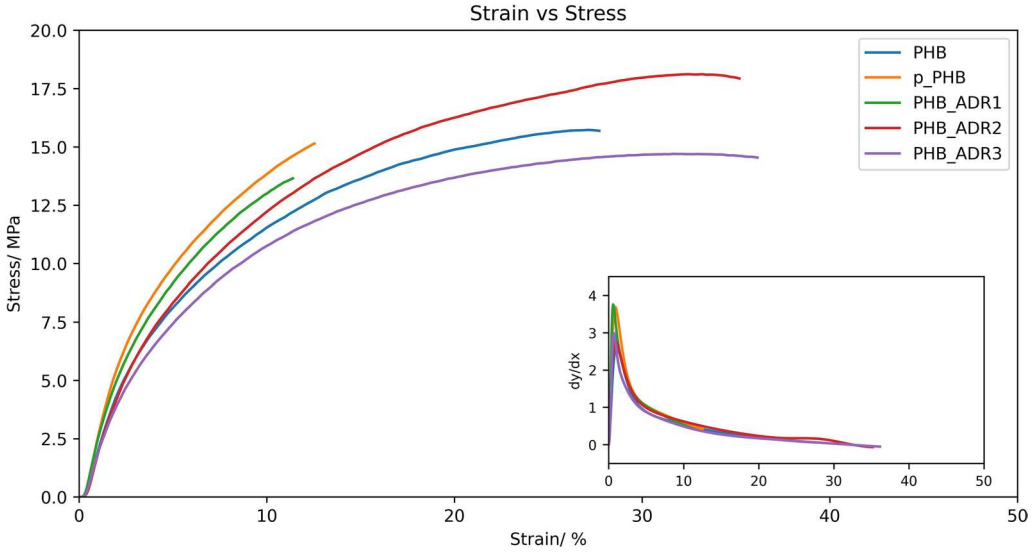

FIGURE 2 | Stress–strain curve and its 1st derivative (inset) of pristine PHB (blue), processed PHB with 0 (orange), 1 (green), 2 (red), 3 (purple) % w/w chain extender.

to turbulent flow profile due to the extremely low viscosity. It was also demonstrated by tan δ that after processing indicated its increasing liquid behavior.

The addition of 1% chain extender does not show any improvement and turbulent flow still occurred at high frequency. Only at 2% and 3% chain extender, the drop in viscosity is counterbalanced to retain 29.8% viscosity of 0.128 Pa s as well as tan δ, suggesting its effect to alleviate PHB degradation. Only a slight increase in the viscosity from 2% to 3% chain extender, which agrees with the tensile test that further higher content of chain extender is in excess, and its effect is plateaued.

The thermal degradation of PHB also reflects on its crystallization and melting (Figure 4, Table 3). One of the key features is the downshift of the melting point with a secondary melting peak. This was also observed in the alcoholysis of PHB with ethylene glycol and glycerol by Lacík et al. The inclusion of a chain extender suppressed the downshifting of the melting point, suggesting reduced formation of PHB oligomers. No significant

TABLE 2 | Young's modulus (E_Y), yield strain (e_Y), yield toughness ($U_{T,Y}$), elongation at break (e_b), ultimate toughness ($U_{T,b}$), and ultimate stress (s_b) of pristine PHB, processed PHB with 0, 1, 2, 3% w/w chain extender.

	E_Y/MPa	ε_Y/%	$U_{T,Y}$/kPa	ε_b/%	$U_{T,b}$/MPa	σ_b/MPa
PHB	226 (29)	1.19 (0.079)	6.63 (0.50)	31.05 (2.58)	3.58 (0.35)	15.5 (0.21)
Processed PHB	312 (44)	0.967 (0.09)	5.22 (0.19)	12.41 (1.00)	1.09 (0.13)	13.7 (0.80)
1% ADR	376 (8.8)	0.612 (0.02)	1.78 (0.28)	11.01 (0.65)	0.97 (0.98)	13.5 (0.39)
2% ADR	320 (30)	0.843 (0.07)	4.71 (0.38)	30.00 (3.66)	3.93 (0.67)	16.8 (0.86)
3% ADR	284 (11)	0.749 (0.02)	2.68 (0.56)	38.79 (2.24)	4.70 (0.35)	14.6 (0.42)

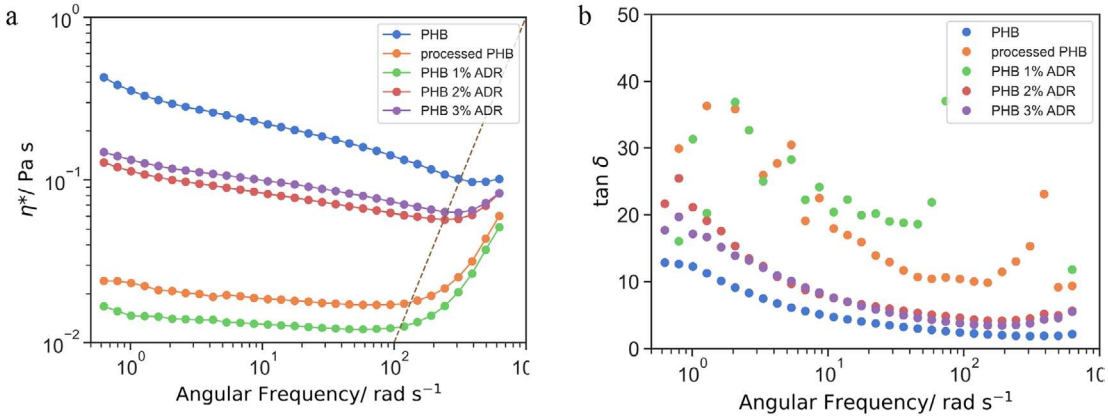

FIGURE 3 | Complex viscosity (a) and tan δ (b) versus angular frequency of pristine PHB (blue), processed PHB with 0 (orange), 1 (green), 2 (red), 3% w/w (purple) chain extender at 180°C.

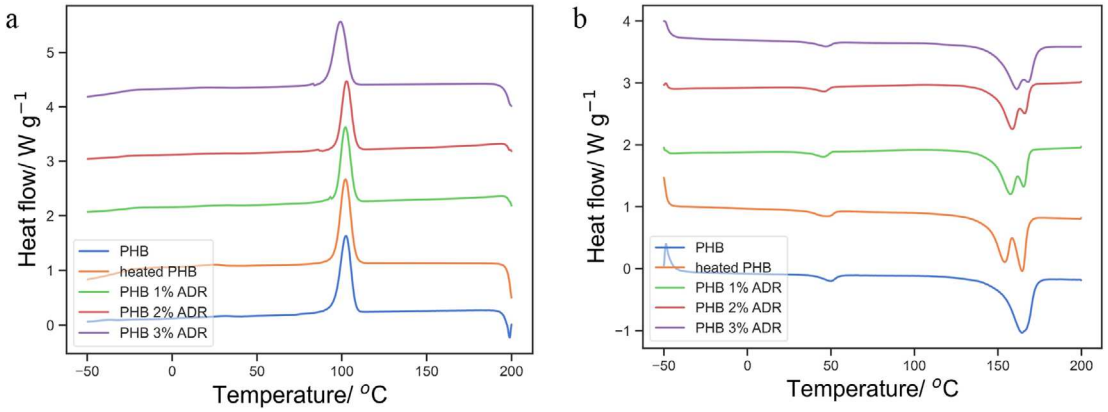

FIGURE 4 | Heat flow from 50°C to 200°C of 2nd cooling (a) and 3rd heating (b) cycle at 15°C min^{-1} of pristine PHB (blue), processed PHB with 0 (orange), 1 (green), 2 (red), 3% w/w (purple) chain extender.

change in the crystallization temperature except when 3% chain extender was added to plasticize PHB against crystallization.

5.2 | PHB/PBAT Blend Compatibilized by Chain Extender

PHB and PBAT are known to be incompatible and phase-separate upon blending. In this study, Joncryl ADR 4468 also acts as a reactive compatibilizer via in situ ring opening of epoxy by both PBAT and PHB, which further generates copolymers of PHB and PBAT that stabilize the polymer blend.

SEM image visualized the degree of phase separation in PHB/PBAT blend (Figure 5). Without compatibilizer, polydisperse droplets of PBAT were observed with a diameter of 10.9 ± 6.32 mm. The introduction of 1% compatibilizer significantly improved the compatibility where phase separation was only observed at the surface, and the size is reduced to approximately 5 mm. At 2 or 3% compatibilizer, no phase separation was observed. Therefore, 2% compatibilizer was selected in the following study.

According to the tensile testing (Figure 6, Table 4), without a compatibilizer, the polymer blend exhibited an elongation at break of 22.06% and a toughness of 1817 kPa. While the addition of the compatibilizer reduced the Young's modulus from 250 MPa to 192, 177, and 182 MPa at 1%, 2%, and 3%, respectively. This indicated the enhanced incorporation of PBAT to reduce the brittleness of PHB in the continuous phase with increasing compatibilizer content up to 2%, and no further improvement at 3%.

After the yielding, the elongation at break and ultimate toughness also reflected the toughening of PHB/PBAT blend. Without compatibilizer, the improvement in e_b, $U_{T,b}$ and s_b were limited

TABLE 3 | Crystallization, melting temperature, their enthalpies and relative % of pristine PHB (corrected for the mass fraction of PHB) of pristine PHB, processed PHB with 0, 1, 2, 3% w/w chain extender.

	T_c/°C	H_c/J g^{-1}	$\%_{c,\,PHB}$	T_m/°C	H_m/J g^{-1}	$\%_{m,\,PHB}$
PHB	103.21	47.28	100%	152.87,163.25	59.08	100%
Processed PHB	103.4	50.2	106.2%	159.36,166.78	54.04	91.5%
1% ADR	103.05	40.84	87.2%	157.95,165.88	47.96	82.0%
2% ADR	103.65	37.4	80.7%	156.28,165.08	51.76	89.4%
3% ADR	101.4	44.68	97.3%	163.69	58	101.1%

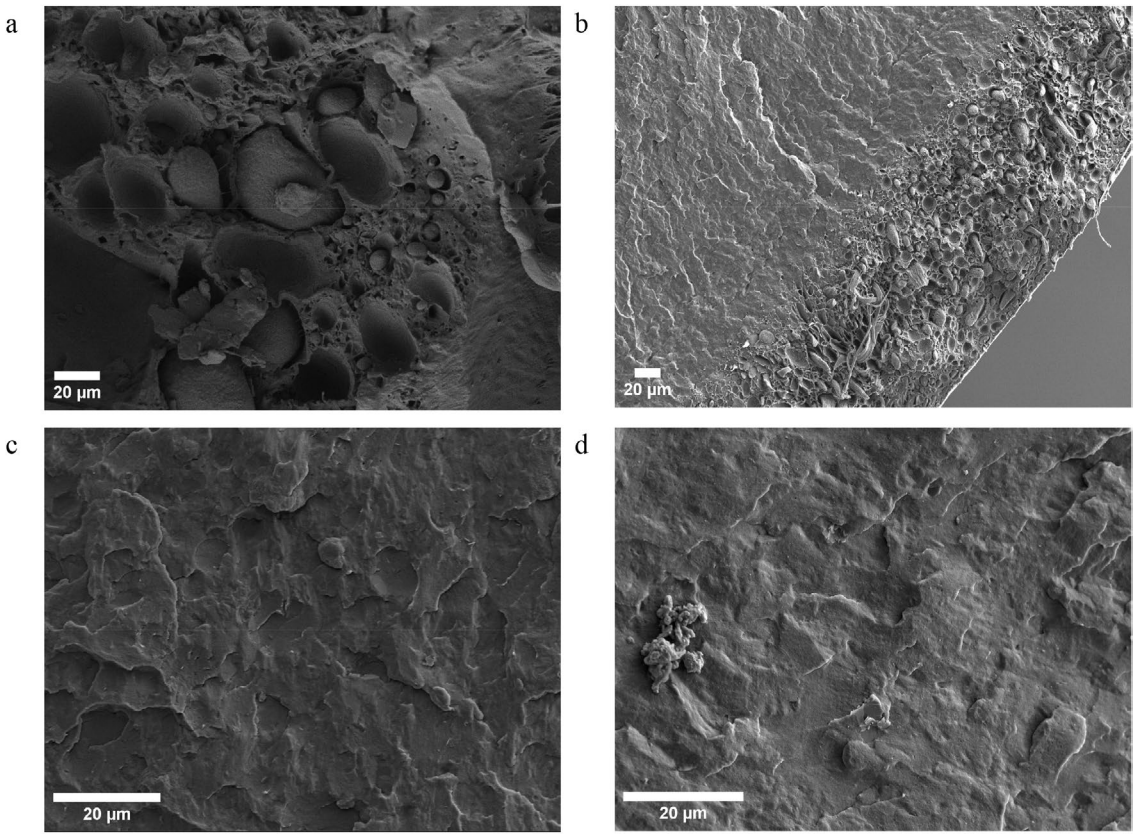

FIGURE 5 | SEM images of 7:3 w/w PHB/PBAT blend with 0 (a), 1 (b), 2 (c), 3% w/w (d) compatibilizer.

due to the predominant PHB in the continuous phase. The addition of compatibilizer massively improved the toughness as more PBAT was incorporated into the continuous phase. It was found that at 2% w/w compatibilizer, the toughening effect is maximum and further increment will be in excess to plasticize the material and reduce both the mechanical strength and elongation. Complementary to SEM imaging, the tensile tests showed the successful incorporation of PBAT to toughen the PHB phase up to 2% compatibilizer where phase separation is minimal and further addition does not have significant improvement. Despite the phase separation of PHB/PBAT blend, the suppression of crystallization was observed in all blends with and without compatibilizer from 103.4°C to 91.51°C, 89.12°C and 89.68°C for 0.1 and 2% w/w compatibilizer (Figure S6, Table 5). At 3% w/w further reduction to 80.93°C was observed, suggesting excessive compatibilizer hindered its crystallization.

Rheology was also performed to elucidate the phase separation in PHB/PBAT blend (Figure 7). G′, G″ and complex viscosity of all blends lie between PHB and PBAT homopolymers, suggesting the enhancement of energy dissipation by PBAT, regardless of the mechanism. A clear peak in tan δ instead of monotonic decay also indicated a secondary relaxation pathway in the polymer blend. This is commonly attributed to interfacial relaxation, where the deformation was counteracted by the interfacial tension against the deformation of phase-separated systems such as polymer blends or emulsions.

Han's plot (log G'' vs. log G') and modified van Gurp-Palmen's plot (tan δ vs. log G*, instead of d for better visuallization) were shown to further visualize the data. For both homopolymers, linear relationship was observed in Han's plot (despite the noise in PHB) whereas clear bending was observed in all polymer

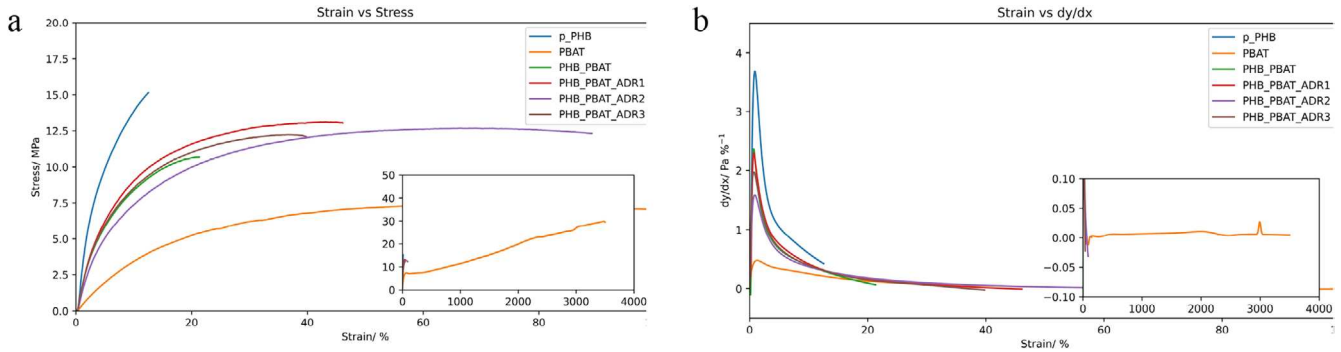

FIGURE 6 | Stress–strain curve (a) and its 1st derivative (b) of processed PHB (blue), PBAT (orange), 7:3 w/w PHB/PBAT blend with 0 (green), 1 (red), 2 (purple), 3(brown)% w/w compatibilizer; inset: Zoom-out of strain from 0 to 4000%.

TABLE 4 | Young's modulus (E_Y), yield strain (e_Y), yield toughness($U_{T,Y}$), elongation at break (e_b), ultimate toughness ($U_{T,b}$), and ultimate stress (s_b) of processed PHB, PBAT, 7:3 w/w PHB/PBAT blend with 0, 1, 2, 3% w/w compatibilizer.

	E_Y/MPa	ε_Y/%	$U_{T,Y}$/kPa	ε_b/%	$U_{T,b}$/MPa	σ_b/MPa
Processed PHB	312 (44)	0.967 (0.090)	5.22 (0.19)	12.41 (1.00)	1.09 (0.13)	13.7 (0.80)
PBAT	46.7 (0.75)	1.14 (0.13)	1.73 (0.68)	3877 (421)	682 (8.9)	29.7 (0.73)
Blank	250 (21)	0.666 (0.034)	1.51 (0.23)	22.06 (0.58)	1.82 (0.16)	11.1 (0.60)
1% ADR	192 (27)	0.813 (0.107)	2.67 (1.06)	49.02 (2.09)	5.20 (0.20)	12.9 (0.23)
2% ADR	177 (23)	0.827 (0.107)	2.48 (0.48)	85.56 (4.61)	9.40 (0.36)	12.4 (0.06)
3% ADR	182 (10.8)	0.758 (0.044)	2.23 (0.62)	43.96 (3.11)	4.19 (0.24)	12.0 (0.17)

TABLE 5 | Crystallization, melting temperature, their enthalpies and relative % of processed PHB (corrected for the mass fraction of PHB) of processed PHB, PBAT and 70:30 w/w PHB/PBAT blend with 0, 1, 2, 3% w/w compatibilizer.

	T_c/°C	H_c/J g^{-1}	$\%_{c,\ PHB}$	T_m/°C	H_m/J g^{-1}	$\%_{m,\ PHB}$
Processed PHB	103.4	50.2	—	152.9, 163.3	59.0	—
PBAT	34.11, 51.38, 71.59	18.8	—	114.7	8.24	—
0% ADR	91.51	28.08	79.9%	162.5, 170.0	28.8	69.6%
1% ADR	89.12	29.52	84.8%	158.9, 167.3	38.4	93.8%
2% ADR	89.68	28.48	82.7%	158.5, 166.8	29.16	71.9%
3% ADR	80.93	25	73.3%	162.6, 171.3	25.04	62.4%

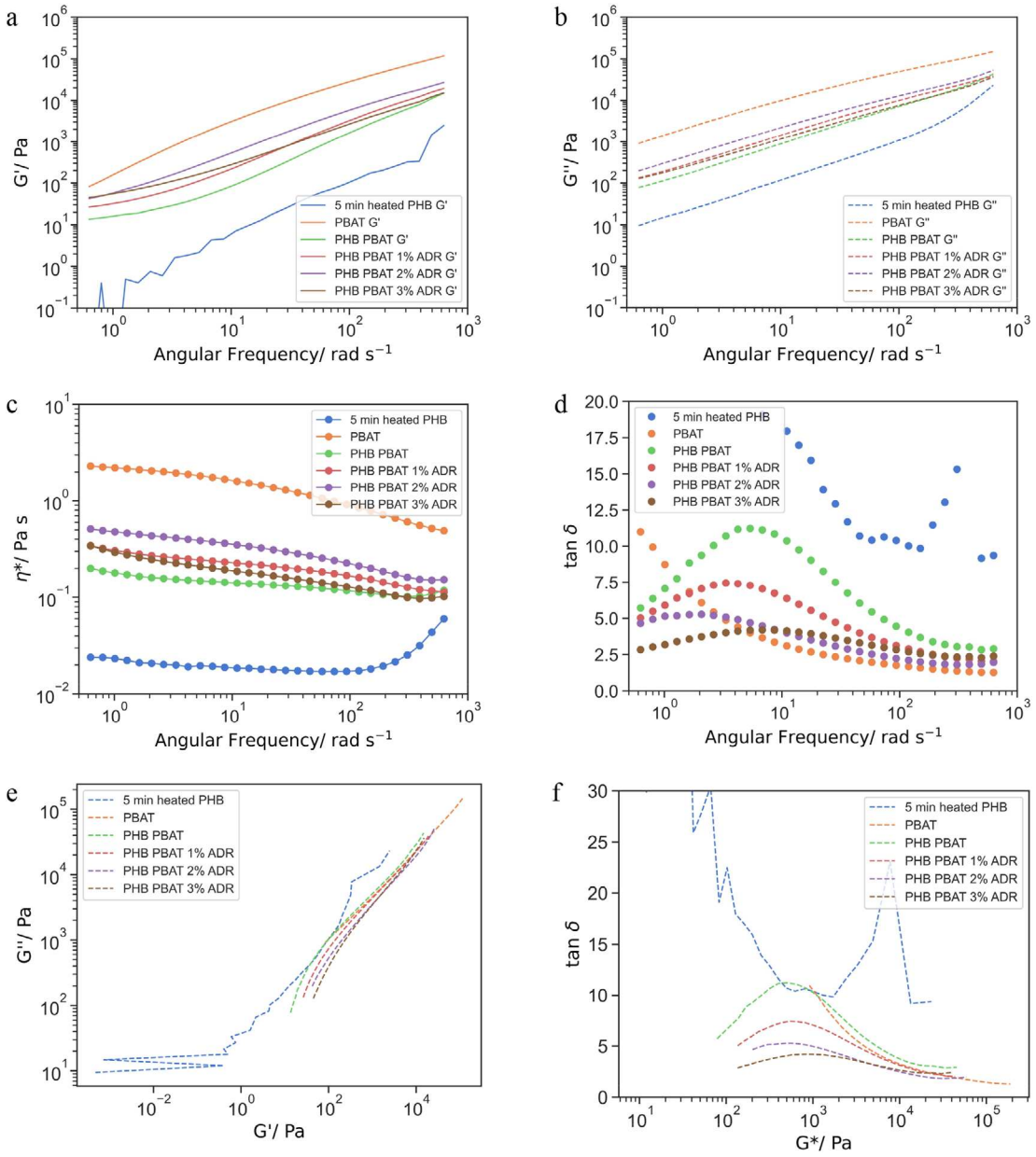

FIGURE 7 | Storage modulus (a), Loss modulus (b), complex viscosity (c), tan δ (d), Han's plot (e) and modified van-Gurp Palmen plot (f) of processed PHB (blue), PBAT (orange), 7:3 w/w PHB/PBAT blend with 0 (green), 1 (red), 2 (purple), 3% w/w (brown) compatibilizer of processed PHB (blue), PBAT (orange), 7:3 w/w PHB/PBAT blend with 0 (green), 1 (red), 2 (purple), 3% w/w (brown) compatibilizer.

blends, which again suggests a secondary relaxation. Modified van Gurp-Palmen's plot qualitatively showed the magnitude of different relaxation mechanisms. It was observed that with increasing compatibilizer peak tan δ was suppressed and shifted towards higher G*. As aforementioned, the interfacial relaxation was the elastic component against the deformation of interfaces. Therefore, the lower tan δ indicates large portion of energy dissipation by this secondary relaxation and its position suggested the contribution to higher modulus. Regarding its structure, it can be rationalized that the increasing compatibilizer (at the same PHB/PBAT ratio) first reduced the individual droplet size, while at constant total droplet volume, and thus enlarge the total interfacial area to contribute the interfacial relaxation.

5.3 | Sequential Blending of Stearic Acid- Surface Modified Cellulose Fiber Into PHB/PBAT Blend

Owing to the strong hydrogen bonding of -OH group, pristine cellulose is incompatible with PHB or PBAT and therefore surface modification with stearic acid was performed to enhance its hydrophobicity. The reaction conditions were optimized to attain significant modification while remain its fiber structure.

The compatibility of MCC in PBAT after surface modification was visually improved with good dispersion in the polymer melt (Figure 8). It was further evidenced by the interfacial microstructure of MCC in PBAT. With pristine MCC, a smooth interface was observed, suggesting poor wettability between

MCC and PBAT, and MCC fiber slipped off upon cracking. After surface modification with stearic acid, a more compact interface was observed which indicates improved interfacial compatibility between MCCSA and PBAT. Peeling was observed at the zoom-in of the void from MCCSA, further suggesting the infiltration of PBAT into MCCSA fiber.

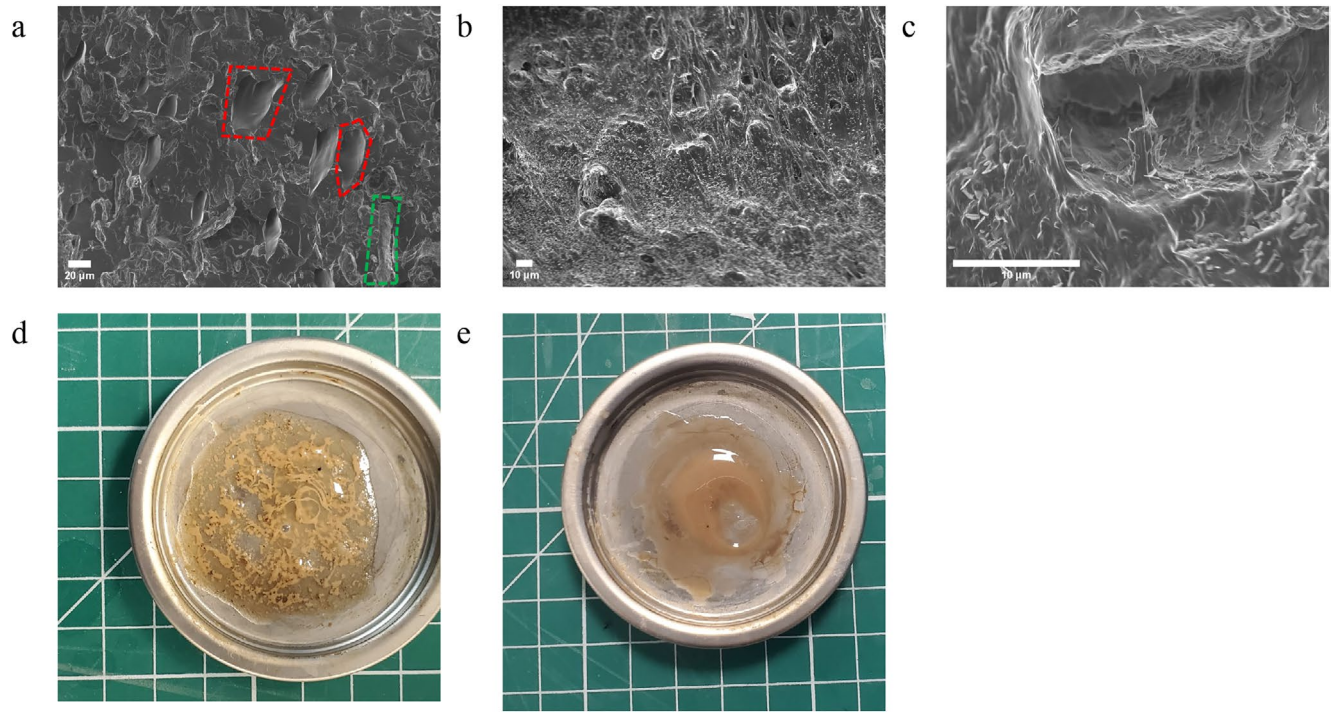

FIGURE 8 | SEM images (top) of 9:1 w/w PBAT/MCC (a) and 9:1 w/w PBAT/MCCSA (b); zoom-in at the void from detached MCCSA (c). Photos of 9:1 w/w PBAT/MCC (d) and 9:1 w/w PBAT MCCSA (e) in melt.

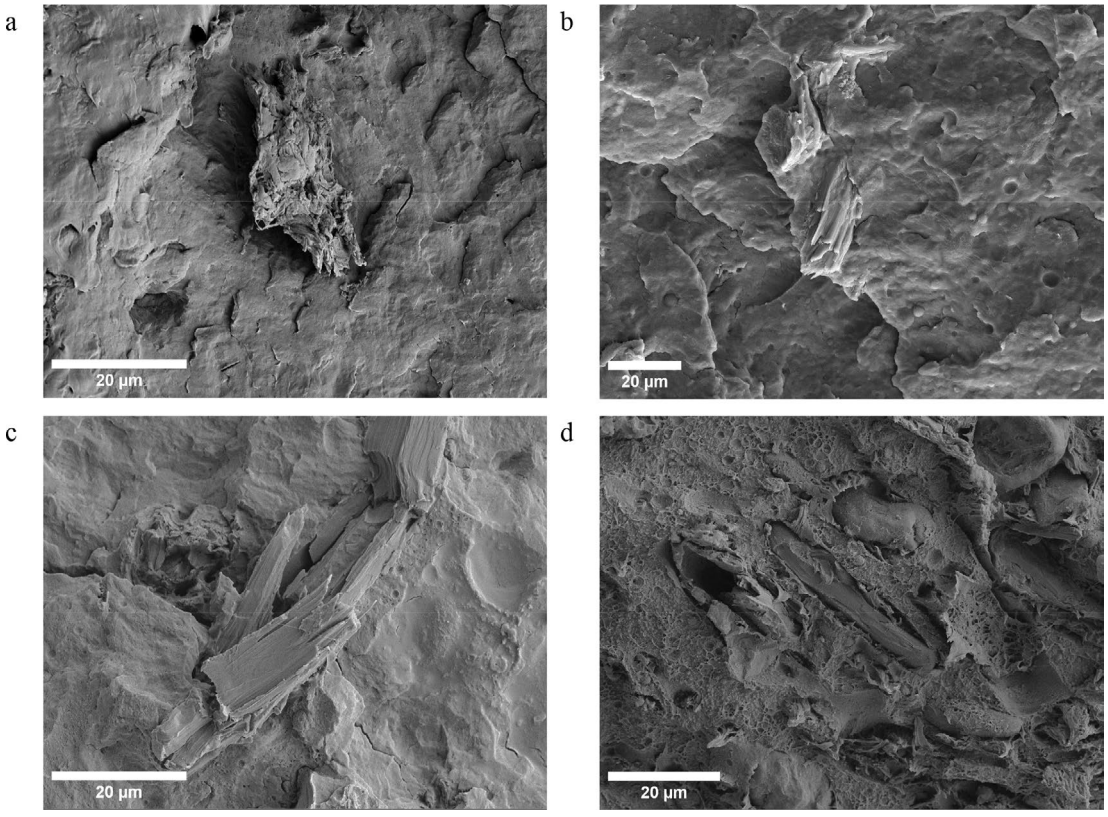

FIGURE 9 | SEM images of (a) PHB/PBAT/3-MCCSA; (b) PHB/(PBAT/3-MCCSA); (c) PHB/PBAT/10-MCCSA; (d) PHB/(PBAT/10-MCCSA).

One of our aims is to investigate whether sequential blending of composite materials will alter the phase separation and thus the mechanical properties of the final material. Herein, PBAT/MCCSA composite was prepared at 10% and 25% MCCSA respectively to create a masterbatch then further blended into PHB with 2% Joncryl ADR 4486 as compatibilizer.

PHB/PBAT/MCCSA was prepared by blending all components in a single step for comparison. The morphology was imaged under SEM (Figure 9). Via batch mixing, poor dispersion was observed in PHB/PBAT/3-MCCSA, and aggregation of MCCSA was also more prominent as the content of MCCSA increased to 10% in PHB/PBAT/10-MCCSA. Via two-step blending, the dispersion and wettability of MCCSA were improved. Elongated phase separation was observed in PHB/(PBAT/10-MCCSA) (25% in PBAT phase) but the MCCSA fiber remained stable without aggregation. It is postulated that MCCSA is less compatible with PHB and remains as aggregates in batch mixing when PHB is the continuous phase. Meanwhile, in sequential mixing, MCCSA is already dispersed in the PBAT phase which is less crystalline and more compatible with stearic acid. During the second blending with PHB, PBAT phase is continuously homogenized, with the aid of compatibilizer, until the MCCSA fiber restrains further droplet breakage, and thus resulting in the elongated phase separation.

Owing to the differences in microstructure, the mechanical properties are also distinctive by sequential blending (Figure 10, Table 6). In all cases, the addition of MCCSA enhanced the rigidity to a different extent, indicated by the higher Young's modulus and shorter elongation at break. No significant differences were observed between batch and sequential blending at 3% MCCSA. However, at 10% MCCSA, PHB/PBAT/10-MCCSA returned to brittle again as pristine PHB (not processed) via one-step batch blending, which means the rigidity by MCCSA fiber counteracts the toughening effect of PBAT. Strikingly, via sequential blending in PHB/(PBAT/10-MCCSA), extended elongation was observed without compromising its strength, where both the stress (14.5 vs. 14 MPa) and elongation at break (42.7% vs. 29.5%) are higher than the batch mixed samples. True reinforcement was achieved via this sequential mixing method.

DSC (Table 7, Figure S6) showed the effect of MCCSA on crystallization and melting of PHB/PBAT composite. All samples showed a lower crystallization temperature but higher melting point than the original blend only; a shoulder at 70°C was also observed in the cooling cycle. Herein, we believe the effect of MCCSA is twofold. It first acts as a physical hindrance for the crystal nucleation which suppresses the crystallization but increases the melting temperature. Second, at higher content, it behaves as a nucleator to promote crystallization at the interface and causes the crystallization temperature to rise back. This was in particular prominent

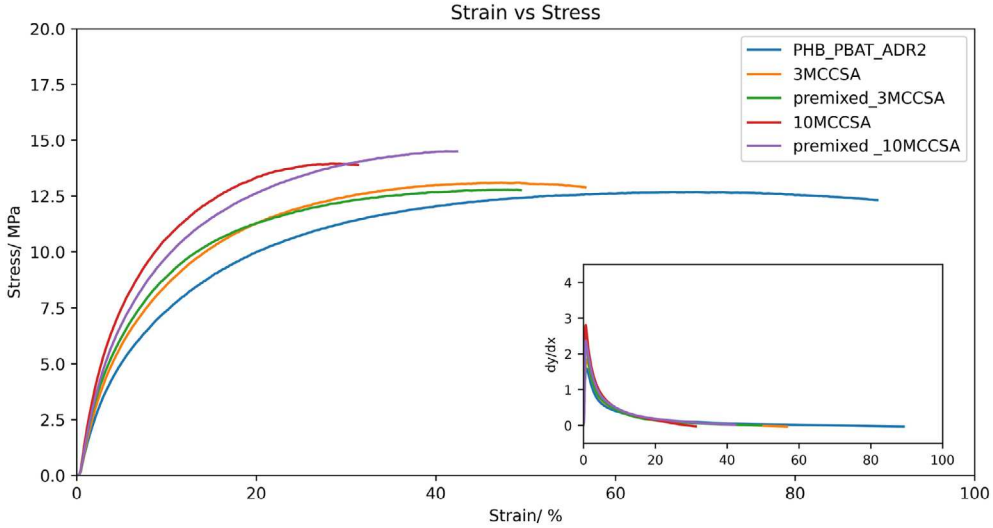

FIGURE 10 | Stress-strain curve and its 1st derivative (inset) of 7:3 w/w PHB/PBAT blend, with 0 (blue), PHB/PBAT/3-MCCSA (orange), PHB/(PBAT/3-MCCSA) (green), PHB/PBAT/10-MCCSA (red), PHB/(PBAT/10-MCCSA) (purple).

TABLE 6 | Young's modulus (E_Y), yield strain (e_Y), yield toughness($U_{T,Y}$), elongation at break (e_b), ultimate toughness ($U_{T,b}$), and ultimate stress (s_b) 7:3 w/w PHB/PBAT blend, PHB/PBAT/3-MCCSA, PHB/(PBAT/3-MCCSA), PHB/PBAT/10-MCCSA and PHB/(PBAT/10-MCCSA).

	E_Y/MPa	ε_Y/%	$U_{T,Y}$/kPa	ε_b/%	$U_{T,b}$/MPa	σ_b/MPa
Without MCCSA	177 (23)	0.827 (0.107)	2.48 (0.48)	85.56 (4.61)	9.40 (0.36)	12.4 (0.06)
3% batch	212 (31)	0.825 (0.095)	2.54 (0.78)	59.01 (1.91)	6.49 (0.22)	12.8 (0.11)
3% premixed	199 (28)	0.919 (0.080)	2.67 (0.80)	56.4 (5.06)	6.03 (0.59)	13.0 (0.19)
10% batch	300 (14)	0.738 (0.044)	2.22 (0.45)	29.5 (1.34)	3.28 (0.12)	14.0 (0.08)
10% premixed	240 (8.8)	0.733 (0.035)	2.00 (0.56)	42.7 (1.79)	4.95 (0.22)	14.5 (0.20)

at 10% MCCSA where most fibers remained in the PHB continuous phase and less effective when MCCSA is premixed in PBAT and eventually less exposed to PHB.

Similar to the polymer blend, a secondary relaxation was signified by the peak of tan δ in all cellulose composites at varied magnitudes and positions (Figure 11). At 3% MCCSA, the

TABLE 7 | Crystallization, melting temperature, their enthalpies and relative % of processed PHB (corrected for the mass fraction of PHB) of 7:3 w/w PHB/PBAT blend, PHB/PBAT/3-MCCSA, PHB/(PBAT/3-MCCSA), PHB/PBAT/10-MCCSA and PHB/(PBAT/10-MCCSA).

	T_c/°C	H_c/J g^{-1}	$\%_{c,\ PHB}$	T_m/°C	H_m/J g^{-1}	$\%_{m,\ PHB}$
Without MCC	89.68	28.48	82.7%	158.54, 166.80	29.16	71.9%
3% batch	87.12	16.56	49.5%	121.31, 159.27, 170.14	24.08	61.1%
3% premixed	87.50	20.84	62.3%	122.81, 163.23, 170.56	23.28	59.1%
10% batch	88.57	25.84	82.4%	123.13, 171.18	24.92	67.5%
10% premixed	88.92	23.48	74.8%	119.85, 161.35, 169.82	25.76	69.8%

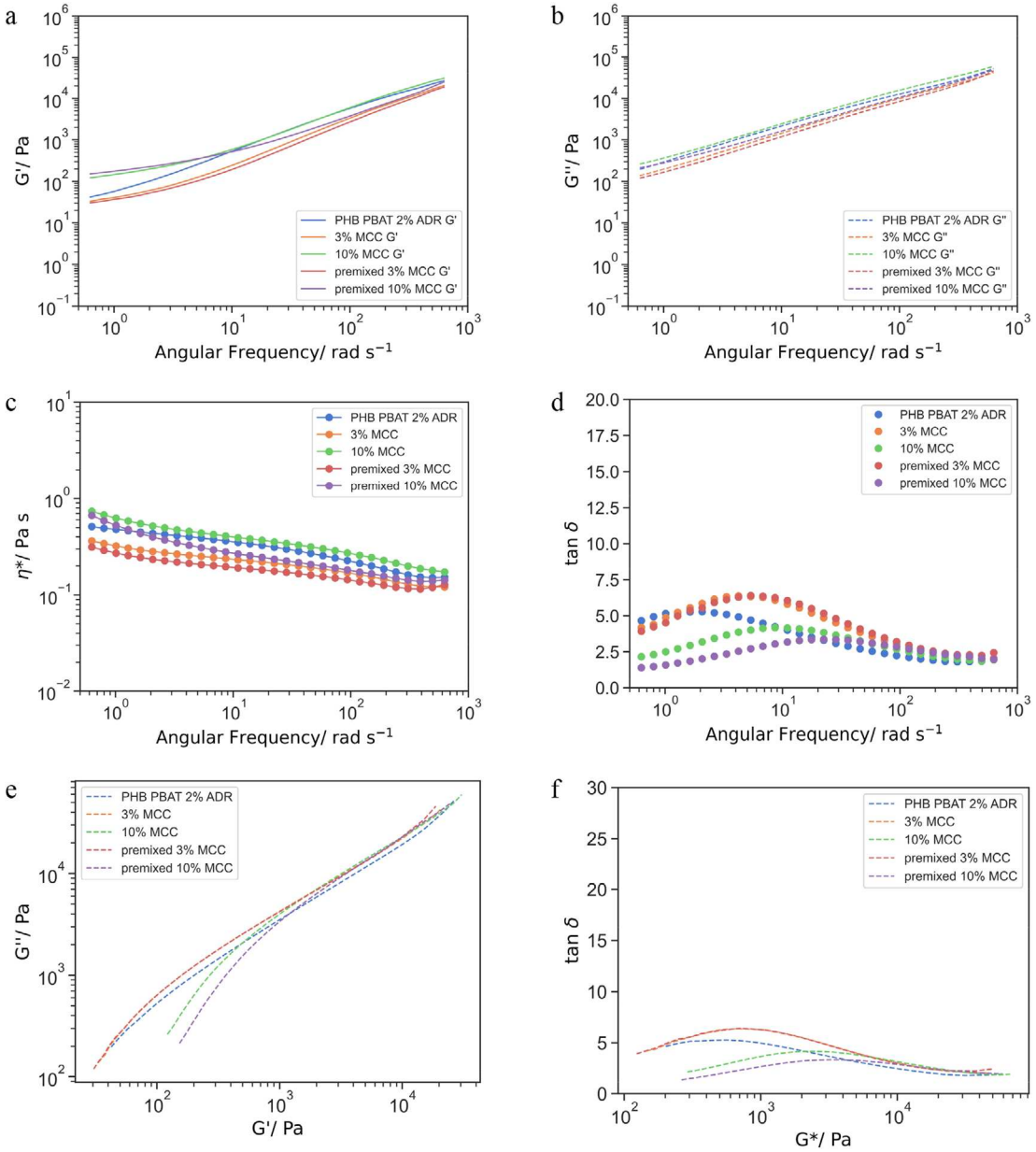

FIGURE 11 | Storage modulus (a), Loss modulus (b), complex viscosity (c), tan δ (d), Han's plot (e) and modified van-Gurp Palmen plot (f) of 7:3 w/w PHB/PBAT blend, PHB/PBAT/3-MCCSA (orange), PHB/PBAT/3-MCCSA (green), PHB/PBAT/10-MCCSA (red), and PHB/(PBAT/10-MCCSA) (purple).

maximum tan δ increased relative to the blend itself, but no significant difference was observed between single batch blending and sequential blending, whereas at 10% MCCSA, suppression of tan δ occurred again to demonstrate its stiffening.

The phase separation is again evaluated from Han's plot and modified van Gurp Palmen's plot. Discontinuity was observed in Han's plot particularly with 10% MCCSA suggesting the distinction of secondary relaxation, whereas no significant difference was observed in 0% and 3% MCC. Modified Van Gurp Palmen plot was more pronounced to distinguish different samples. From 0% to 3% MCCSA, the peak tan δ increased and shifted to higher modulus suggesting the broadening of interfacial relaxation. However, no significant difference between batch and sequential blending. At 10% MCCSA, the peak tan δ was further suppressed and shifted towards higher G*, and by sequential mixing of MCCSA showed the lowest tan δ at highest G*, which means the best dissipation against deformation. Complementary to the tensile test and SEM, the improved dispersion of MCCSA by sequential blending and selective concentration at PBAT phase facilitate dissipation and therefore reinforcing the material by maximizing the surface area between MCCSA and the polymer as well as selectively toughen PBAT phase.

From these results, we have observed improved reinforcement by sequential blending of MCCSA into PBAT to make a masterbatch then to PHB, as compared to one-step batch blending. We postulate that the reinforcement originated from the preferential localization of MCCSA via different blending procedures. In one-step blending, stearic acid is incompatible with PHB as the continuous phase and therefore MCCSA remains as aggregates instead of being exfoliated, resulting in poor mechanical properties due to limited interfacial interaction with MCCSA. In contrast, MCCSA is well dispersed in the PBAT phase by making a masterbatch of PBAT/MCCSA. During the second blending with PHB, PBAT along with MCCSA is gradually broken down to smaller droplets until it is confined by well-dispersed MCCSA, as shown by the elongated phase separation. Via this sequential blending, the improved dispersion and interfacial dissipation between PHB and PBAT, then PBAT and MCCSA, significantly enhanced the reinforcement of the PHB/PBAT/MCCSA composite.

6 | Conclusion

This study shows the optimization and characterization of PHB/PBAT reinforced with modified cellulose fiber. The thermal stability of PHB was firstly overcome by using Joncryl ADR 4468 as a chain extender and compatibilizer to maintain its processibility in melt state and prepare homogeneous PHB/PBAT blend for toughness. Then the reinforcement by the addition of stearic acid-modified cellulose fiber was investigated. It was found that one-step batch processing results in poor dispersion of cellulose fiber in the polymer blend, making it brittle. In contrast, sequentially adding premixed PBAT/cellulose fiber with PHB offered good dispersion and locally templated PBAT phase to achieve better reinforcement with higher stiffness while retaining higher elongation. This signifies the control in microstructure and optimization of mechanical properties by changing the processing sequence even from the same compositions and opens an avenue to process PHB blend and its composite for different materials.

Author Contributions

Wai Hin Lee: conceptualization, methodology, software, data curation, investigation, validation, formal analysis, visualization, project administration, writing – original draft, writing – review and editing. **Jagroop Pandhal:** funding acquisition, writing – review and editing, project administration. **Ipsita Roy:** writing – review and editing, project administration, funding acquisition. **Chaoying Wan:** conceptualization, methodology, supervision, funding acquisition, visualization, project administration, resources, writing – original draft, writing – review and editing.

Acknowledgments

The authors would like to thank the financial support from EPSRC (EP/X021491/1).

Funding

This work was supported by the Engineering and Physical Sciences Research Council.

Data Availability Statement

The data that support the findings of this study are available from the corresponding author upon reasonable request.

References

1. P. A. Holmes, *Developments in Crystalline Polymers*, ed. D. C. Bassett (Springer Netherlands, 1988), 1–65.

2. C. P. Holmes, "Separation Process," 1989, US 4,910,145.

3. "3-Hydroxybutyrate Polymer Composition," **1990**, 5,061,743.

4. "Polyhydroxyalkanoate (Pha) Dispersion and Preparation Method Therefor," **2022**, EP 4 379 001 A1.

5. J. M. Herring and A. Webb, "3-Hydroxybutyrate Polymer Composition," **1991**, US5061743A.

6. G. D. Figuly, "Processing of Polyhydroxyalkanoates Using a Nucleant and a Plasticizer," **2004**, US6774158B2.

7. S. Nguyen, G. E. Yu, and R. H. Marchessault, "Thermal Degradation of Poly(3-Hydroxyalkanoates): Preparation of Well-Defined Oligomers," *Biomacromolecules* 3 (2002): 219–224.

8. T. Omura, T. Goto, A. Maehara, S. Kimura, H. Abe, and T. Iwata, "Thermal Degradation Behavior of Poly[(R)-3-Hydroxybutyrate-Co-4-Hydroxybutyrate]," *Polymer Degradation and Stability* 183 (2021): 109460.

9. J. Y. Choi, J. K. Lee, Y. You, and W. H. Park, "Epoxidized Polybutadiene as a Thermal Stabilizer for Poly(3-Hydroxybutyrate). II. Thermal Stabilization of Poly(3-Hydroxybutyrate) by Epoxidized Polybutadiene," *Fibers and Polymers* 4 (2003): 195–198.

10. S. N. Lee, M. Y. Lee, and W. H. Park, "Thermal Stabilization of Poly(3-Hydroxybutyrate) by Poly(Glycidyl Methacrylate)," *Journal of Applied Polymer Science* 83 (2002): 2945–2952.

11. Y. Shaked, H. Dodiuk, S. Kenig, and S. McCarthy, "The Effect of Hyperbranched Polymers on Processing and Thermal Stability of Biodegradable Polyesters," *Polymer Engineering & Science* 49 (2009): 559–566.

12. T. H. Steinke, H.-H. Görtz, J. Ahlers, F. Gruber, and G. Skupin, "Biodegradable Polymer Mixture," 2015, US8937135B2.

13. A. Javadi, A. J. Kramschuster, S. Pilla, J. Lee, S. Gong, and L.-S. Turng, "Processing and Characterization of Microcellular PHBV/PBAT Blends," *Polymer Engineering & Science* 50 (2010): 1440–1448.

14. A. K. Pal, F. Wu, M. Misra, and A. K. Mohanty, "Reactive Extrusion of Sustainable PHBV/PBAT-Based Nanocomposite Films With Organically Modified Nanoclay for Packaging Applications: Compression Moulding vs. Cast Film Extrusion," *Composites Part B: Engineering* 198 (2020): 108141.

15. E. Pesaranhajiabbas, A. K. Mohanty, and M. Misra, "Reactive Extrusion of Biodegradable Poly(3-Hydroxybutyrate-Co-3-Hyrdoxyvalerate) and Poly(Butylene Adipate-Co-Terephthalate) Blends: Toward a Toughening Approach," *ACS Applied Polymer Materials* 7 (2025): 2439–2450.

16. A. R. M. Costa, L. T. A. Reul, F. M. Sousa, E. N. Ito, L. H. Carvalho, and E. L. Canedo, "Degradation During Processing of Vegetable Fiber Compounds Based on PBAT/PHB Blends," *Polymer Testing* 69 (2018): 266–275.

17. R. Hoffmann, D. D. S. Morais, C. J. F. Braz, et al., "Impact of the Natural Filler Babassu on the Processing and Properties of PBAT/PHB Films," *Composites Part A: Applied Science and Manufacturing* 124 (2019): 105472.

18. D.-F. Hou, P.-Y. Li, K. Zhang, et al., "Insight Into the Feasibility of Fatty Acyl Chlorides With 10–18 Carbons for the Ball-Milling Synthesis of Thermoplastic Cellulose Esters," *Biomacromolecules* 25 (2024): 1923–1932.

19. H. S. Kwatra, J. M. Caruthers, and B. Y. Tao, "Synthesis of Long Chain Fatty Acids Esterified Onto Cellulose via the Vacuum-Acid Chloride Process," *Industrial and Engineering Chemistry Research* 31 (1992): 2647–2651.

20. C. J. Maim, J. W. Mench, D. L. Kendall, and G. D. Hiatt, "Aliphatic Acid Esters of Cellulose. Preparation by Acid-Chloride-Pyridine Procedure," *Industrial and Engineering Chemistry* 43 (1951): 684–688.

21. A. N. Netravali, Y. Zhong, and N. V. Patil, Modified Cellulosic Compositions Having Increased Hydrophobicity and Processes for Their Production," **2022**, US11326303B2.

22. M. Bernheim, H. Meindl, and P. Rohringer, "Process for Sizing Paper or Cardboard With Anionic Hydrophobic Sizing Agents and Cationic Retention Aids," 1988, Us4735685a.

23. T. Lindstrom and G. Soderberg, "On the Mechanism of Sizing With Alkylketene Dimers: Part 1. Studies on the Amount of Alkylketene Dimer Required for Sizing Different Pulps," *Nordic Pulp & Paper Research Journal* 1 (1986): 26–33.

24. E. Guidotti and M. Jabbari, "Method for Producing a Cellulose Product and a Cellulose Product," 2025, US12312745B2.

25. S. Gong, B. Li, H. Liu, et al., "Facile Preparation of Eco-Friendly Plastic From Rosin Modified Microcrystalline Cellulose for Food Packaging," *Industrial Crops and Products* 221 (2024): 119370.

26. D. Pasquini, E. de M. Teixeira, A. A. da S. Curvelo, M. N. Belgacem, and A. Dufresne, "Surface Esterification of Cellulose Fibres: Processing and Characterisation of Low-Density Polyethylene/Cellulose Fibres Composites," *Composites Science and Technology* 68 (2008): 193–201.

27. J. E. Sealey, G. Samaranayake, J. G. Todd, and W. G. Glasser, "Novel Cellulose Derivatives. IV. Preparation and Thermal Analysis of Waxy Esters of Cellulose," *Journal of Polymer Science Part B: Polymer Physics* 34 (1996): 1613–1620.

28. L. Huang, Q. Wu, Q. Wang, R. Ou, and M. Wolcott, "Solvent-Free Pulverization and Surface Fatty Acylation of Pulp Fiber for Property-Enhanced Cellulose/Polypropylene Composites," *Journal of Cleaner Production* 244 (2020): 118811.

29. L. Elias, F. Fenouillot, J. C. Majeste, and P. Cassagnau, "Morphology and Rheology of Immiscible Polymer Blends Filled With Silica Nanoparticles," *Polymer* 48 (2007): 6029–6040.

30. L. Wei, W. Jiang, K. Goh, and Y. Chen, "Mechanical Reinforcement of Polyethylene Using n-Alkyl Group-Functionalized Multiwalled Carbon Nanotubes: Effect of Alkyl Group Carbon Chain Length and Density," *Polymer Engineering and Science* 54 (2014): 336–344.

31. R. Tchoudakov, O. Breuer, M. Narkis, and A. Siegmann, "Conductive Polymer Blends With Low Carbon Black Loading: Polypropylene/Polyamide," *Polymer Engineering & Science* 36 (1996): 1336–1346.

32. D. Yan, X. Li, H.-L. Ma, X.-Z. Tang, Z. Zhang, and Z.-Z. Yu, "Effect of Compounding Sequence on Localization of Carbon Nanotubes and Electrical Properties of Ternary Nanocomposites," *Composites Part A: Applied Science and Manufacturing* 49 (2013): 35–41.

Supporting Information

Additional supporting information can be found online in the Supporting Information section. **Figure S1:** DSC thermogram of the 2nd cooling and 3rd heating cycle of pristine PHB as received. Yellow box indicated the integrated area to calculate the crystallinity relative to it in other samples. **Figure S2:** SEM images of cotton fiber (microcrystalline cellulose) after esterification with stearic acid in 0 (top left), 0.33 (top right), 1 (bottom left) and 3.5 (bottom right) eqv of OH groups at 130°C for 3 h. **Figure S3:** FTIR spectra of cotton fiber (microcrystalline cellulose) after esterification with stearic acid in 0, 0.33, 1 and 3.5 eqv of OH groups at 130°C for 3 h. **Figure S4:** SEM images of cotton fiber (microcrystalline cellulose) after esterification with stearic acid in 1 eqv of OH groups at 130°C for 1 h (top left), 2 h (top right), 3 h (bottom left) and 16 h (bottom right). **Figure S5:** FTIR spectra of cotton fiber (microcrystalline cellulose) after esterification with stearic acid in 1 eqv of OH groups at 130°C for 1 h (top left), 2 h (top right), 3 h (bottom left) and 16 h (bottom right). **Figure S6:** Heat flow from 50°C to 200°C of 2nd cooling (a) and 3rd heating (b) cycle at 15°C min^{-1} of pristine PBAT (blue), processed PHB (orange), 7:3 w/w PHB/PBAT blend with 0 (green), 1 (red), 2 (purple) and 3% w/w (brown) compatibilizer. **Figure S7:** Heat flow from 50°C to 200°C of 2nd cooling (a) and 3rd heating (b) cycle at 15°C min^{-1} of 7:3 w/w PHB/PBAT blend(blue), PHB/PBAT/3-MCCSA (orange), PHB/PBAT/3-MCCSA (green), PHB/PBAT/10-MCCSA (red), and PHB/(PBAT/10-MCCSA) (purple).